

Single point mutations in the helicase domain of the NS3 protein enhance dengue virus replicative capacity in human monocyte-derived dendritic cells and circumvent the type I interferon response

G. F. Silveira,^{*1} D. M. Strottmann,^{*1}
L. de Borba,^{*2} D. S. Mansur,[†]
N. I. T. Zanchin,[‡] J. Bordignon^{*} and
C. N. Duarte dos Santos^{*}

^{*}Laboratório De Virologia Molecular, Instituto Carlos Chagas, Curitiba, Brasil, [†]Laboratório De Imunobiologia, Universidade Federal De Santa Catarina, Trindade, Florianópolis, Brasil, and [‡]Laboratório De Proteômica E Engenharia De Proteínas, Instituto Carlos Chagas, Curitiba, Brasil

Accepted for publication 3 September 2015
Correspondence: C. N. Duarte dos Santos,
Instituto Carlos Chagas, FIOCRUZ, Rua
Prof. Algacyr Munhoz Mader 3775, CIC,
81350-010, Curitiba, Brasil.
E-mail: clsantos@tecpar.br

¹G. F. Silveira and D. M. Strottmann
contributed equally to the present study.

²Current address: Luana de Borba, Fundación
Instituto Leloir, Ave. Patricias Argentinas 435,
C1405BWE, Buenos Aires, Argentina.

Introduction

Dengue is a serious worldwide public health problem that is endemic in more than 100 countries in Latin America, Africa, Southeast Asia and the Pacific Islands. The World Health Organization estimates that approximately 400 million people are infected annually, and that a total of 2.5 billion people live in areas posing a risk of infection [1–3].

Dengue virus (DV) has a positive single-stranded RNA (ssRNA) belonging to the genus *Flavivirus* of the *Flaviviridae* family. The DV genome encodes a single open reading frame (ORF) that is flanked by two untranslated regions (5' and 3' UTRs) [4]. The infectious RNA is surrounded by a nucleocapsid (C protein) as well as a lipid membrane and

Summary

Dengue is the most prevalent arboviral disease worldwide. The outcome of the infection is determined by the interplay of viral and host factors. In the present study, we evaluated the cellular response of human monocyte-derived DCs (mdDCs) infected with recombinant dengue virus type 1 (DV1) strains carrying a single point mutation in the NS3_{hel} protein (L435S or L480S). Both mutated viruses infect and replicate more efficiently and produce more viral progeny in infected mdDCs compared with the parental, non-mutated virus (vBACDV1). Additionally, global gene expression analysis using cDNA microarrays revealed that the mutated DVs induce the up-regulation of the interferon (IFN) signalling and pattern recognition receptor (PRR) canonical pathways in mdDCs. Pronounced production of type I IFN were detected specifically in mdDCs infected with DV1-NS3_{hel}-mutated virus compared with mdDCs infected with the parental virus. In addition, we showed that the type I IFN produced by mdDCs is able to reduce DV1 infection rates, suggesting that cytokine function is effective but not sufficient to mediate viral clearance of DV1-NS3_{hel}-mutated strains. Our results demonstrate that single point mutations in subdomain 2 have important implications for adenosine triphosphatase (ATPase) activity of DV1-NS3_{hel}. Although a direct functional connection between the increased ATPase activity and viral replication still requires further studies, these mutations speed up viral RNA replication and are sufficient to enhance viral replicative capacity in human primary cell infection and circumvent type I IFN activity. This information may have particular relevance for attenuated vaccine protocols designed for DV.

Keywords: dendritic cells, dengue virus, NS3 helicase, type I IFN, viral replicative capacity

membrane (M) and envelope (E) proteins [5]. Upon infection of host cells, the DV ssRNA serves as a template for the translation of three structural (C, prM and E) and seven non-structural (NS1, NS2A, NS2B, NS3, NS4A, NS4B and NS5) proteins and subsequently as the template for RNA synthesis [5]. The structural proteins are essential components of the virion and play roles in viral entry, fusion and assembly. In contrast, the functions of the non-structural proteins are not completely understood; however, all these proteins have been implicated in DV replication, and several play important roles in immune evasion [6–10]. In particular, NS3 and NS5 are multifunctional proteins within the major enzymatic components of the viral replication complex [11,12]. The NS3

protein specifically contains a serine protease domain at its N-terminus and a helicase domain at the C-terminus. The latter domain possesses three different enzymatic activities: RNA triphosphatase (RTPase), RNA helicase and nucleoside triphosphatase (NTPase), which play a role in ssRNA virus replication [12,13]. Furthermore, NS3 has a pivotal function in viral particle assembly; namely, in the cleavage of the C-prM precursor by the NS2B-NS3 protease [14,15].

The four dengue serotypes are referred to as DV1, DV2, DV3 and DV4 and are closely related [16–18]. Infection with any one of the four DVs can cause a spectrum of clinical manifestations, ranging from self-limiting non-symptomatic disease to dengue fever (DF), with symptoms including headache, fever, arthralgia, myalgia, nausea, vomiting and/or rashes [19,20]. DF can evolve into dengue haemorrhagic fever (DHF), which may progress to dengue shock syndrome (DSS) and patient death. DHF involves bleeding, thrombocytopenia and plasma leakage, which are attributed to increased vascular permeability [20,21]. Although DV strains that correlate directly with disease severity have not been identified, differences in the intrinsic biological properties and the replication rate of various DV strains are known to influence the pathogenesis of dengue [22].

In natural infection, dendritic cells (DCs) are one of the primary cells targeted by DV infection, and these cells represent a central link between the innate and the adaptive immune responses [23,24]. DCs can sense viral RNA using a unique mechanism due to their expression of pattern recognition receptors (PRRs), such as Toll-like receptors (TLRs) and/or retinoic acid-inducible gene (RIG)-like receptors (RLRs) [25,26]. ssRNA sensing by PRR stimulates a pathway that culminates in the production of type I interferon (IFN) (IFN- α and IFN- β), which induces an anti-viral state in cells via induction of the expression of IFN-stimulated genes (ISGs) that prevent viral replication [27]. However, it is noteworthy that certain DV strains have evolved several escape mechanisms to subvert and evade the human innate immune response mediated by type I IFN. For example, DV-2 (particularly the 16681 and NGC strains) non-structural proteins are associated with inhibition of type I IFN action. NS2A, NS4A and NS4B interfere specifically with this signalling pathway, thereby inhibiting the Janus kinase–signal transducer and activator of transcription (JAK–STAT) pathway [28]. In addition, NS2B/3 protease directly cleaves the stimulator of the IFN gene (STING), leading to suppression of type I IFN production [29,30], and NS5 mediates STAT-2 degradation [31,32]. However, these escape mechanisms appear to be strain-dependent and not serotype-specific [33].

In a previous study, we constructed recombinant DV1 viruses carrying a single point mutation (L435S or L480S) affecting the NS3_{hel} protein, which were identified during a dengue neuropathogenesis study. The recombinant viruses (vBACDV1-NS3₄₃₅ and vBACDV1-NS3₄₈₀) exhibited

enhanced replicative capacity both *in vivo* (murine model) and *in vitro* (human and mosquito cell lines) [34]. In mice, a significant increase in the mortality rate was observed after infection with the vBACDV1-NS3₄₃₅ and vBACDV1-NS3₄₈₀ recombinant viruses compared with the vBACDV1 parental strain, suggesting that the emergence of a high degree of replication early observed during viral infection may play an important role in DV pathogenesis [34]. In the present study, to evaluate the cellular response in an environment correlated closely with natural infection, we analysed the *in-vitro* infection of human monocyte-derived DCs (mdDCs) with recombinant vBACDV1-NS3₄₃₅ or vBACDV1-NS3₄₈₀ or the parental strain of virus. Significant amounts of type I IFN were produced by the mdDCs, but the anti-viral activity of type I IFN was not sufficient to abrogate cell infection with the NS3-recombinant strains. The data presented here suggest that the NS3 helicase domain is an important virulence factor, and this information contributes to our understanding of DV pathogenesis and may provide the basis for rational vaccine design strategies.

Materials and methods

Human primary dendritic and cell lines cultures

Peripheral blood mononuclear cells from 30 healthy volunteers were collected by peripheral venue puncture after informed consent forms were signed, and the cells were used to generate mdDCs. The experimental protocol was approved by the FIOCRUZ Research Ethics Committee (number 514/09). Mononuclear cells were separated by density gradient centrifugation using lymphocyte separation medium (Lonza, Walkersville, MD, USA), and monocytes (CD14⁺ cells) were purified by magnetic immunosorting (Miltenyi Biotec, Auburn, CA, USA), according to the manufacturer's recommendations. The plastic adherence technique was also employed for monocyte purification (1.5 h in a plastic bottle with non-supplemented RPMI-1640 medium (Lonza). The monocytes were cultured for 6–7 days in RPMI-1640 medium supplemented with 100 ng/ml interleukin (IL)–4 (PeproTech, Rocky Hill, NJ, USA), 50 ng/ml granulocyte–macrophage colony-stimulating factor (GM-CSF; PeproTech) and 10% fetal bovine serum (FBS), 100 IU/ml penicillin, 100 μ g/ml streptomycin, 0.25 μ g/ml amphotericin B and 2 mM L-glutamine (GIBCO-BRL, Grand Island, NY, USA).

Immunophenotyping was determined using antibodies against CD1a, CD11c, CD11b, CD209, humal leucocyte antigen D-related (HLA-DR) and CD14 that were conjugated to the fluorescein isothiocyanate (FITC), phycoerythrin (PE), peridinin chlorophyll (PerCp), allophycocyanin (APC), APC-H7 and AmCyan fluorochromes, respectively (Becton Dickinson, San Jose, CA, USA). After 30 min of incubation at 37°C, the cells were washed with phosphate-buffered saline (PBS; Lonza), and the staining was evaluated

using a fluorescence activated cell sorter (FACS)Canto II (Becton Dickinson). The analysis was performed in a flow cytometry facility (RPT08L PDTIS) at Carlos Chagas Institute—Fiocruz/PR. The acceptable phenotypical values for the cells were greater than 85% for CD1a⁺, CD11c⁺, CD11b⁺, CD209⁺ and HLA-DR⁺ and below 5% for CD14⁺ (Fig. S1).

C6/36 cells (*Aedes albopictus*; American Type Culture Collection, Manassas, VA, USA; CRL-1660) were grown at 28°C in Leibovitz L-15 medium supplemented with 5% FBS, 0.26% tryptose and 25 µg/ml gentamicin (all reagents from GIBCO-BRL).

Vero E6 cells (African Green monkey kidney cells, a subclone of Vero 76; CRL-1586) were propagated at 37°C in Dulbecco's modified Eagle's F-12 medium (DMEM-F12) supplemented with 10% FBS and 10 µg/ml penicillin and streptomycin (all reagents were purchased from GIBCO-BRL).

Viruses

The recombinant viruses vBACDV1, vBAC-NS3₄₃₅ and vBAC-NS3₄₈₀ used in this study were obtained from an infectious clone of DV1 [34]. To generate working virus stocks, three rounds of infection in the C6/36 mosquito cell line at multiplicities of infection (MOIs) of 0.01 were performed during 5 days of infection. The cell culture supernatants were then titrated using focus-forming assays [35] and were used to infect mdDCs. A mock-infected preparation was obtained from non-infected C6/36 cells using the same protocol.

Recombinant vesicular stomatitis virus (VSV)-green fluorescent protein (GFP) was kindly provided by Dr João Trindade Marques of the Federal University of Minas Gerais (UFMG). To grow the VSV-GFP, Vero E6 cells were infected with viruses at an MOI of 0.01, and the cell culture supernatants were recovered at 24 h post-infection (hpi). VSV-GFP titres were determined by a plaque assay using Vero E6 cells. Briefly, monolayers of Vero E6 cells in 24-well plates were infected with serially diluted samples of VSV-GFP in serum-free DMEM-F12. After the cells were incubated in a 5% CO₂ incubator for 1 h at 37°C, the inoculum was removed and a 1.6% carboxymethyl cellulose (CMC) complete DMEM overlay was added. The cell monolayers were then incubated for 24 h prior to counterstaining the plaques using a crystal violet solution. VSV-GFP at an MOI of 5 was then used to infect mdDCs. A mock-infected preparation was obtained from non-infected Vero E6 cells using the same protocol.

Viral genome sequencing

To confirm the identity of the viruses and to avoid any spurious mutations, complete viral genome sequences were determined after mdDC infection. Viral RNA was purified

from the supernatant of the infected cells using the QIAamp Viral RNA Mini Kit (Qiagen, Valencia, CA, USA). The resulting RNA was reverse-transcribed with ImProm-II Reverse Transcriptase (Promega, Madison, WI, USA) in the presence of random primers (100 pmol/µl; Invitrogen, Carlsbad, CA, USA), and the entire genome was amplified with specific primers for nucleotide sequencing by polymerase chain reaction (PCR) (Macrogen Sequencing Service, Seoul, South Korea).

mdDC infection and type I IFN production

To evaluate the susceptibility of mdDCs to infection with DV strains, 5.0×10^5 cells (from six different healthy donors) were infected with vBACDV1, vBAC-NS3₄₃₅ or vBAC-NS3₄₈₀ or were mock infected at an MOI of 5 for 2 h at 37°C and 5% CO₂. After incubation, the cells were washed with fresh medium and plated in 24-well plates in 0.5 ml supplemented RPMI-1640. Cells and supernatants were recovered at 8, 24 and 48 hpi. The supernatants were used to determine viral titres via focus-forming assay and to determine type I IFN levels using cytometric bead array technology (Becton Dickinson) for IFN-α and a VeriKineTM human IFN-β enzyme-linked immunosorbent assay (ELISA) Kit (PBL, Piscataway, NJ, USA) for IFN-β, according to the manufacturer's instructions. The infected cells were also assessed by flow cytometry. To determine the number of infected mdDCs, cells were washed with PBS and blocked with 5% FBS and 1% human serum type AB (Lonza) for 20 min at room temperature (RT). The cells were then fixed and permeabilized with a Cytofix/Cytoperm kit (Becton Dickinson) for 20 min at RT. Next, the cells were washed and stained with the monoclonal antibody (mAb) 4G2 (flavivirus-specific) in Perm/Wash buffer for 20 min at 37°C. After washing, the cells were incubated with secondary antibody in Perm/Wash buffer (donkey anti-mouse polyclonal antibody conjugated to Alexa Fluor 488; eBioscience, San Diego, CA, USA) for 30 min. The cells were also stained with a monoclonal antibody (mAb) against CD11c (conjugated to PE fluorochrome; Becton Dickinson). Finally, the cells were washed in PBS and analysed using a FACSCanto II (Becton Dickinson). The cytometry data files were analysed with FlowJo software 2.2.8 (Tree Star Inc., Ashland, OR, USA) and DIVA software (Becton Dickinson).

To determine the binding affinity of the recombinant viruses for mdDCs, cells infected with vBACDV1, vBAC-NS3₄₃₅ or vBAC-NS3₄₈₀ or mock-infected controls were incubated at an MOI of 5 for 2 h at 4°C. The cells were then washed with ice-cold PBS to remove unbound virus, followed by incubation as described previously. The percentage of infection and the viral genome were then assessed by flow cytometry and quantitative reverse transcription-polymerase chain reaction (qRT-PCR), respectively, in six cultures.

Microarray experiments, bioinformatic analyses and qRT-PCR

Cultures of mdDCs from 10 different donors were mock-infected or infected with vBACDV1, vBAC-NS3₄₃₅ or vBAC-NS3₄₈₀ at an MOI of 5 for 2 h in the absence of FBS. After the viral inocula were removed, the cells were cultured in RPMI-1640 plus 10% FBS, 100 IU/ml penicillin, 100 µg/ml streptomycin, 0.25 µg/ml amphotericin B and 2 mM L-glutamine (GIBCO-BRL) [36]. The cells were then collected at 8, 24 and 48 hpi, and total RNA was extracted using the RNeasy Mini Kit (Qiagen), according to the manufacturer's recommendations. RNAs from all 10 mdDC groups were pooled (75 µg of each) for the microarray experiments and compared with RNAs from mock-infected cells using Human Gene 1.0 ST version 1 array GeneChip slides from Affymetrix (Santa Clara, CA, USA). The RNA pools were processed according to the manufacturer's recommendations regarding amplification, *in-vitro* transcription, purification, tagging, hybridization and slide-scanning (GeneChip[®] Scanner 3000).

The .cel extension files, which contain images depicting the expression levels detected during the scanning process, were analysed for quality using Expression Console software (Affymetrix). The same software was used to normalize the data by the Robust Multi-array Average (RMA) method [37]. Log ratios between vBACDV1-, vBAC-NS3₄₃₅- or vBAC-NS3₄₈₀-infected mdDCs and mock-infected mdDCs intensity signal values were generated, and a list of differentially expressed genes was obtained using the criterion of a fold change (FC) ≥ 2. Data clustering was performed using Cluster version 3.0 software with a Euclidian distance. The Tool for Analysis of GO Enrichments (TANGO) function in Expander software was used to obtain gene ontologies (GOs) with a statistical enhancer value of 0.05. The NCBI Entrez Gene database (www.ncbi.nlm.nih.gov) and the Gene Ontology database (www.geneontology.org) were used to define the most relevant cell signalling and metabolic pathways during mdDC infection with vBACDV1, vBAC-NS3₄₃₅ or vBAC-NS3₄₈₀. To determine the canonical pathways for different modulated genes, the expression data were analysed using Ingenuity Pathway Analysis (IPA) software (Redwood City, CA, USA). The entire set of supporting microarray data was deposited in the Gene Expression Omnibus (GEO) public database under registration number GSE50698.

To confirm the microarray results, we selected three modulated genes for qRT-PCR analysis [myxovirus resistance 1 (MX), eukaryotic translation initiation factor 2-alpha kinase 2 (EIF2ak2) and STAT-2; the primer sequences are presented in Table S1]. mdDCs from six different donors were mock-infected or infected with vBACDV1, vBAC-NS3₄₃₅ or vBAC-NS3₄₈₀ at an MOI of 5 for 8, 24 or 48 hpi. Briefly, total RNA was extracted with an RNeasy Mini Kit (Qiagen), according to the manufacturer's recom-

mendations, and cDNA was generated using random primers (Invitrogen) and reverse transcriptase (Promega). qRT-PCR amplifications were performed using the SYBR Green Master Mix (Applied Biosystems, Inc., Grand Island, NY, USA). The following cycles were used for DNA amplification: 50°C for 2 min; 96°C for 10 min; and 40 cycles of 96°C for 15 s, 59°C for 30 s and 72°C for 1 min. Melting curves were used to verify product specificity. The house-keeping gene 18S was also included to normalize the amplification reaction [36]. Gene modulation was calculated by adapting the $2^{-\Delta\Delta CT}$ method described by Livak *et al.* in 2001 [38].

The same qRT-PCR protocol as described above was used to determine the mRNA levels for DV1-NS3 and other IFN-related human genes, including the genes encoding TLR-3, TLR-7, IFN-α, IFN-β, ISG56, I kappa B alpha (IκBα), RIG-I and melanoma differentiation-associated gene 5 (MDA5). For these quantifications, mdDCs were infected with a mutated (vBAC-NS3₄₃₅ or vBAC-NS3₄₈₀) or parental (vBACDV1) DV strain at an MOI of 5, and the cells were recovered at 2, 8, 24 and 48 hpi for total RNA extraction.

Type I IFN functional experiments

To evaluate the role of type I IFN throughout mdDC infection with the DV parental strain or a mutated strain, six mdDC cultures were infected at an MOI of 5 for 2 h. The cultures were then incubated with RPMI medium (untreated cells), recombinant IFN-α (rIFN-α; 200 U/ml; Blausiegel, São Paulo, SP, Brazil), anti-human IFN-α/β receptor chain 2 neutralizing antibody (α-IFN-R2; 3.0 µg/ml; PBL, Piscataway, NJ, USA) or isotype control (mouse anti-GFP mAb; 3.0 µg/ml). The level of rIFN-α used was determined in a dose-response experiment (Fig. S2), and the levels of α-IFN-R2 used were based on the manufacturer's recommendation. After 8, 24 and 48 hpi, the percentage of infected mdDCs was determined by cytometry, as described above, for all types of mdDC infection.

NS3_{hel} expression and purification

Plasmid DNA (pET28a; Novagen, Madison, WI, USA) containing recombinant sequences from the NS3_{hel} DENV-1 FGA/89 strain (NS3_{hel} WT) (GenBank Accession number AF226687) or the mutant NS3_{hel} 435Mut (GenBank Accession number AF226686.1) NS3_{hel} 480Mut (GenBank Accession number EF122231.1) or NS3_{hel} 200Mut (enzymatically inactive K200A mutant) was transformed into *Escherichia coli* Rosetta-gami 2 (DE3) host cells. We constructed the NS3_{hel} 200Mut mutant for use as a negative control for the ATPase assay. It was shown previously that substitution of the corresponding K200 residue in DV-2 greatly reduces ATPase and RNA helicase activities [39]. Cultures were induced at 30°C in the presence of 0.4 mM IPTG for 5 h. The cells were then resuspended in buffer A

[50 mM phosphate buffer (pH 7.4), 0.5 M NaCl and 10 mM imidazole] and lysed using an M-110L Microfluidizer processor (Microfluidics, Newton, MA, USA) at 18 000 psi. The lysate was clarified by centrifugation at 30 000 *g* for 20 min at 4°C, and additional centrifugation at 50 000 *g* for 30 min was performed after addition of 1% of streptomycin sulphate (Sigma, Saint Quentin Fallavier, France) to the supernatant to remove nucleic acid precipitates. The supernatant was then filtered through a 0.22 µm syringe filter and purified by metal affinity using a HisTrap HP column (GE Healthcare, Piscataway, NJ, USA) and an ÄKTA Prime Fast Protein Liquid Chromatography (FPLC) system (GE Healthcare). Proteins were eluted using a linear gradient ranging from 40 to 500 mM imidazole equilibrated in buffer A. The fractions containing Trx-His₆-NS3_{hel} were diluted 1 : 7 with buffer B [20 mM HEPES (pH 7.4)] and were purified further by ion exchange chromatography using a HiTrap Heparin HP column (GE Healthcare). NS3_{hel} was then eluted using a linear gradient ranging from 0.05 to 1.0 M NaCl equilibrated in buffer B and was analysed by sodium dodecyl sulphate–polyacrylamide gel electrophoresis (SDS-PAGE) (13%). Protein quantification was performed at least three times using a Qubit Protein Assay Kit (Invitrogen).

Nucleotide hydrolysis assay

ATP hydrolysis was determined using a colorimetric assay measuring inorganic phosphate (Pi) release [40]. In accordance with [41], we used a 3'-overhang double-stranded RNA (dsRNA) substrate to stimulate NTPase activity. For annealing, the complementary oligonucleotides RF (5'-AGCACCGUAAAGACGC3') and R3'-R (5'-GCGUCUUACGGUGUCUAAAACAAAACAAAACAAAACAAAAC-3') were mixed at a 1 : 1 molar concentration in buffer containing 2 mM HEPES (pH 7.0), 50 mM NaCl, 0.1 mM EDTA and 0.01% SDS (w/v). The oligonucleotide mix was then heated at 95°C for 5 min, followed by a linear decrease in the temperature to 20°C to allow gradual annealing. The dsRNA was purified using illustra MicroSpin G-25 Columns (GE Healthcare) and was then quantified spectrophotometrically. RNA-stimulated ATPase activity was determined as described below, using different concentrations of dsRNA or adenosine-5'-triphosphate (ATP) (Affymetrix). For the ATPase assay, purified recombinant NS3_{hel} variants at a concentration of 80 nM diluted in protein buffer [50 mM Tris-HCl, (pH 7.5), 300 mM NaCl and 10% glycerol] were incubated for 30 min at 27°C in an equal volume of phosphate-free reaction buffer [50 mM Tris-HCl (pH 7.5), 25 mM KCl, 2.5 mM MgCl₂ and 200 nM purified dsRNA]. Reactions were started by the addition of different amounts of ATP (0.2–1.2 mM) to the media. After 10 min at 27°C, 200 µl of freshly prepared malachite green reagent (0.027% malachite green, 0.95% ammonium molybdate in 6 N HCl and

0.38% polyvinyl alcohol) was added to each reaction mixture to form a complex with free orthophosphate. The mixture was then incubated for 5 min at RT, after which 25 µl of 34% sodium citrate was added to stop colour development. The release of Pi was monitored by measuring the absorbance at 650 nm in a Synergy H1 Hybrid Multi-Mode Microplate Reader (BioTek, Winooski, VT, USA). NS3_{hel} inactive mutant (K200A) was used as a baseline for the reactions. Standard curves were generated by diluting phosphate buffer to known phosphate concentrations (one standard curve for each experiment), and the absorbance values obtained for inactive NS3_{hel} (K200A) was used as a reference (negative control). The samples' absorbance values were then fitted to the linear portion of the standard curve to extrapolate the molar concentration of released phosphate in each sample. Assays were carried out in triplicate to evaluate the initial rates of ATP hydrolysis. The results were fitted to the Michaelis–Menten equation by non-linear regression to determine the constants V_{max} , K_{cat} and K_M using GraphPad Prism version 5 software (GraphPad Software, San Diego, CA, USA).

Statistical analysis

All data are reported as means and scatter dot-plot graphics. In addition, all data were submitted to two-way analysis of variance (ANOVA) followed by Bonferroni correction. The level of significance for these analyses was established to be $P \leq 0.05$. The analyses were performed using GraphPad Prism version 3.0 software.

Results

A high capacity for viral replication is an important virulence factor involved in the pathogenesis of dengue, and viruses with a more efficient replication cycle tend to cause more severe symptoms [24,42]. To determine the susceptibility of human mdDCs to infection, cells derived from six different donors were infected with the parental strain (vBACDV1) or with the vBAC-NS3₄₃₅ or vBAC-NS3₄₈₀-mutated strain, or were mock-infected, and were then subjected to flow cytometry analysis at 8, 24 and 48 hpi. Representative cytometry zebra plots used to determine the percentage of infected mdDCs are presented in Fig. 1a. The DV1-NS3_{hel} mutant yielded a higher percentage of CD11c⁺/4G2⁺ cells (mdDCs⁺/DV⁺) compared with the parental strain and the mock control at 48 hpi (Fig. 1a,b). To determine the replication rates of the DV1 variants in mdDCs, DV1-NS3 gene expression was analysed. At 2 hpi, no difference was observed between the parental and the mutant strains (Fig. 1c), suggesting no differences in viral attachment and adsorption to mdDCs, but a significant increase in DV1-NS3 gene expression was observed over the time-points analysed for the mutant strains compared with the parental strain (Fig. 1c). Viral progeny were also

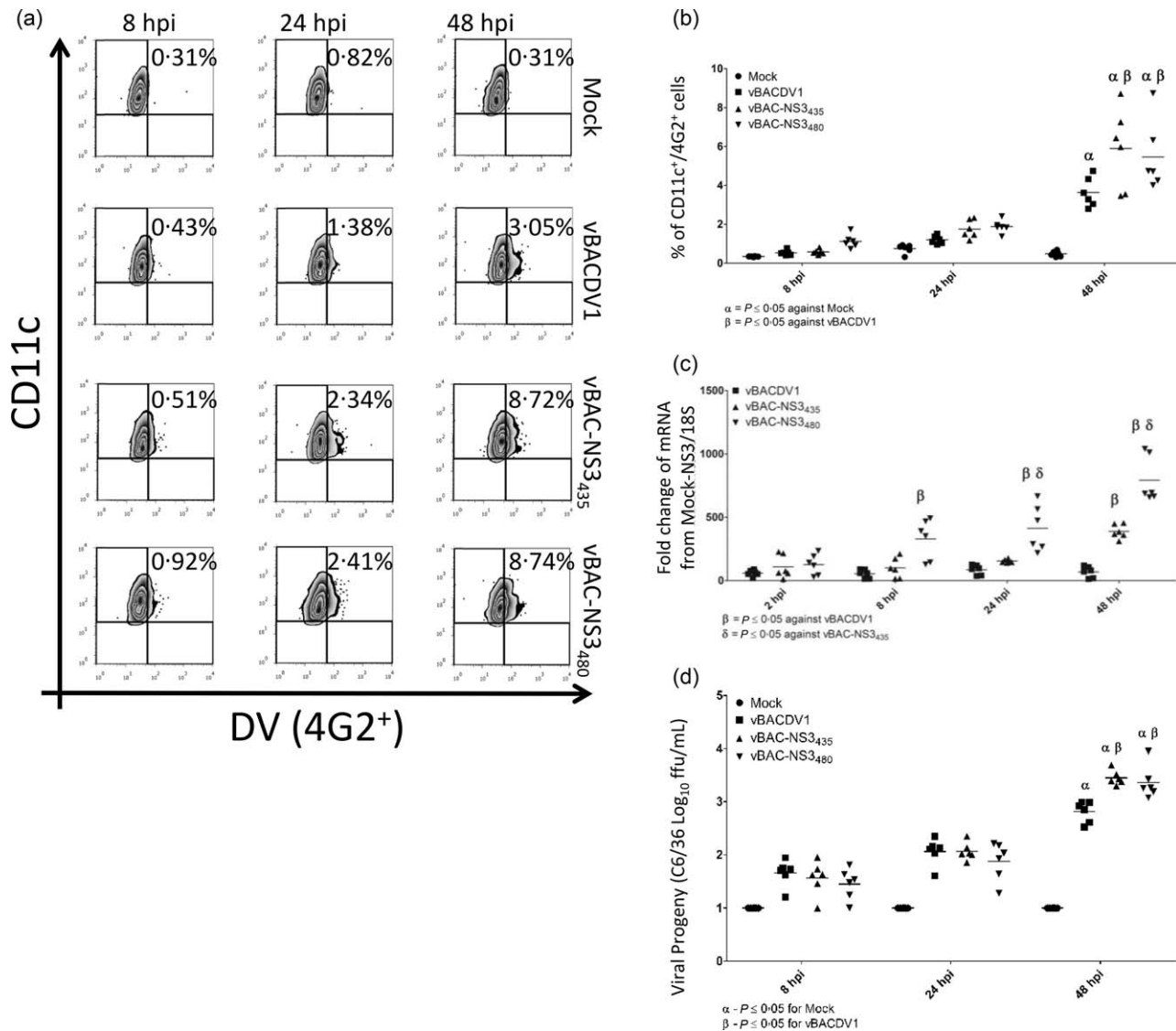


Fig. 1. A single point mutation in the dengue virus type 1 (DV1)-non-structural protein 3 (NS3)_{hel} protein enhances viral replicative capacity during monocyte-derived dendritic cell (mdDC) infection. Immature mdDCs were infected (multiplicity of infection of 5) with one of three strains of DV1 (vBACDV1, vBAC-NS3435 or vBAC-NS3480) or were mock-infected. The mdDCs were then analysed at three different time-points: 8, 24 and 48 h post-infection (hpi). (a) A representative example of dot-plot and gating strategy for analysis of cells from one of six different donors. Flow cytometry determination was performed for mdDCs [anti-CD11c monoclonal antibody (mAb)-positive cells] infected with DV (4G2 anti-flavivirus E protein mAb). (b) Percentage of mdDCs from six different donors that were positive for DV infection, as determined by flow cytometry. (c) Detection of DV non-structural protein 3 (NS3) mRNA in mdDC pellets. The results are expressed as the fold change (FC) between cells infected with an NS3-mutated strain and mock-infected cells and were normalized to the 18S housekeeping gene using the $2^{-\Delta\Delta CT}$ method. (d) Viral progeny were detected by immunodetection of focus-forming units per ml in the supernatant of mdDCs infected with DV. $\alpha = P \leq 0.05$ compared with mock; $\beta = P \leq 0.05$ compared with vBACDV1; $\delta = P \leq 0.05$ compared with vBAC-NS3₄₃₅.

detected in the supernatant of infected mdDCs using a focus-forming immunoassay in C6/36 cells. The results confirm that the increases in the percentage of 4G2 antibody-positive cells and in viral RNA levels were the result of a productive viral infection (Fig. 1d). The presence of the mutations L435S and L480S (corresponding to the vBAC-NS3₄₃₅ and vBAC-NS3₄₈₀ strains, respectively) was also assessed by sequencing the complete viral genomes

present in virus particles in the supernatants of the infected mdDCs. No spurious mutations were observed in the samples, indicating that the observed results were linked exclusively to the contributions of the L435S and L480S mutations (data not shown). The data suggest that in mdDCs, viruses harbouring L435S or L480S exhibit increased viral replicative capacity compared with the parental virus. Although no mutations have been mapped

Table 1. Kinetic parameters for adenosine triphosphatase (ATPase) hydrolysis of recombinant dengue virus type 1 (DV1) non-structural protein 3 (NS3)_{hel} variants

	V_{\max} ($\mu\text{mol}/\mu\text{mol NS3}_{\text{hel}}/\text{min}$)	K_m (mM)	K_{cat} (s^{-1})	K_{cat}/K_m ($10^3 \text{ M}^{-1} \text{ s}^{-1}$)
NS3 _{hel} WT	10.04 \pm 3.44	0.1864 \pm 0.08197	0.1255 \pm 0.01352	0.6733 \pm 0.27714
NS3 _{hel} 435 _{Mut}	17.49 \pm 2.69	0.1682 \pm 0.03822	0.2186 \pm 0.01119	1.2996 \pm 0.24125
NS3 _{hel} 480 _{Mut}	24.80 \pm 4.44	0.2685 \pm 0.06604	0.3100 \pm 0.02246	1.1546 \pm 0.21322

Parameter values correspond to the non-linear analysis from the substrates curves of three independent experiments.

to the structural proteins of the parental and mutated viruses, we conducted mdDC infection at 4°C to exclude any possible differences in the entry steps for the viruses. There were no differences in the percentages of infected cells (Fig. S3a) or in viral RNA synthesis (Fig. S3b) at 6 hpi, suggesting that the same level of infection was observed at the initial time-points for all three viruses; an increase in viral RNA replication was observed only at later time-points in cells infected with the mutated strains.

DV1-NS3_{hel} drives RNA-unwinding activity using free energy derived from the hydrolysis of nucleotide triphosphate, and it has been suggested that this function facilitates the activity of RNA-dependent RNA polymerases during viral genome replication [39]. To evaluate how the non-conservative amino acid substitutions at residues 435 and 480 could regulate DV1 replication positively, we used a recombinant helicase domain of the NS3 protein to measure the effects of these genetic determinants on RNA-dependent ATPase activity. We observed that 3'-overhang dsRNA is an allosteric activator of DV1-NS3_{hel}, increasing the rate of ATP hydrolysis in presence of 100–600 nM short dsRNA (data not shown). For comparative analysis of ATPase assay results, all experiments were performed to obtain substrate curves for ATP hydrolysis in the presence of 200 nM dsRNA and to determine the catalytic parameters according to the V_{\max} , K_M and K_{cat} values (Fig. S4 and Table 1). The presence of a serine residue at positions 435 or 480 promoted an increase in the turnover rate constant (K_{cat}), enhancing the catalytic efficiency of the enzymes (K_M/K_{cat}) by 1.9- and 1.7-fold, respectively. The results suggest that single point mutations in NS3_{hel} induce a positive effect on genome replication by modulating ATPase activity. We then evaluated how this enhanced replication affected the DC response to infection.

DCs sense viral infection via PRRs [43]. To evaluate whether an increase in viral replicative capacity would induce differential RNA sensing and responses by mdDCs infected with DV1 strains, cultures from 10 healthy volunteers were infected with vBACDV1, vBAC-NS3₄₃₅ or vBAC-NS3₄₈₀ or were mock-infected for 8, 24 or 48 h, and the mRNA pools from the mdDCs were used for microarray hybridization. For each infection condition, the following gene expression was observed in the mdDCs: 125 genes up-regulated and 250 genes down-regulated for vBACDV1 (Table S2), 302 genes up-regulated and 144 genes down-

regulated for vBAC-NS3₄₃₅ (Table S3) and 199 genes up-regulated and 131 genes down-regulated for vBAC-NS3₄₈₀ (Table S4). The microarray data were confirmed by qRT-PCR analyses of the MX1, STAT-2 and EIF2ak2 genes in six new cultures of infected mdDCs (Fig. S5). Analyses to determine the enhancement of canonical genetic pathways with P -values $\geq 5 \log_2$ for differentially expressed genes in infected mdDCs revealed up-regulation of innate immune response-related groups of genes, including genes related to IFN signalling (P -value $\geq 8 \log_2$), PRRs (P -value $\geq 6 \log_2$) and activation of IFN regulatory factors (IRFs) by cytokine PRRs (P -value $\geq 6 \log_2$). The same differentially expressed canonical pathways were observed when comparing cultures infected with the parental strain or a mutated strain. In total, 38% (187 genes) of all differentially expressed genes were observed in mdDCs infected with the parental strain or a mutated strain (Fig. 2a), confirming that infection with mutated strains and infection with the parental strain induce similar gene modulation.

The canonical pathways with higher differential gene expression in DV1-infected mdDCs were the IFN signalling and PRR pathways. Analyses of 30 modulated PRR-related genes with high variation between DV-infected cells and mock-infected cells revealed that the expression of the TLR-3 and TLR-7 genes (Fig. 2b, blue arrows) was up-regulated in mdDCs infected with the DV1-NS3_{hel}-mutated strains, especially at 24 hpi (Fig. 2b). The TLR-3 and TLR-7 gene expression observed via microarray was confirmed by qRT-PCR analysis of six new cultures of DV1-infected mdDCs at 2, 8, 24 and 48 hpi (Fig. 2c,d). The same infected cultures were also analysed for differential modulation of other genes that play a role in the PRR pathway. RIG-I (Fig. S6a) and MDA5 (Fig. S6b) gene expression was not modulated differentially in mdDCs infected with the mutated and parental strains, suggesting that TLR was the main PRR stimulated in response to infection with the mutated strains. PRR stimulation culminates in the activation of transcription factors such as nuclear factor kappa light-chain-enhancer of activated B cells (NF- κ B) and IRF3/7. Mutated viruses also differentially increased transcription of the IRF3 target IFN-stimulated gene 56 (ISG56) (Fig. 2e) and the NF- κ B target I κ B α (Fig. 2f) in mdDCs. We next evaluated whether this differential gene expression resulted in IFN- α production.

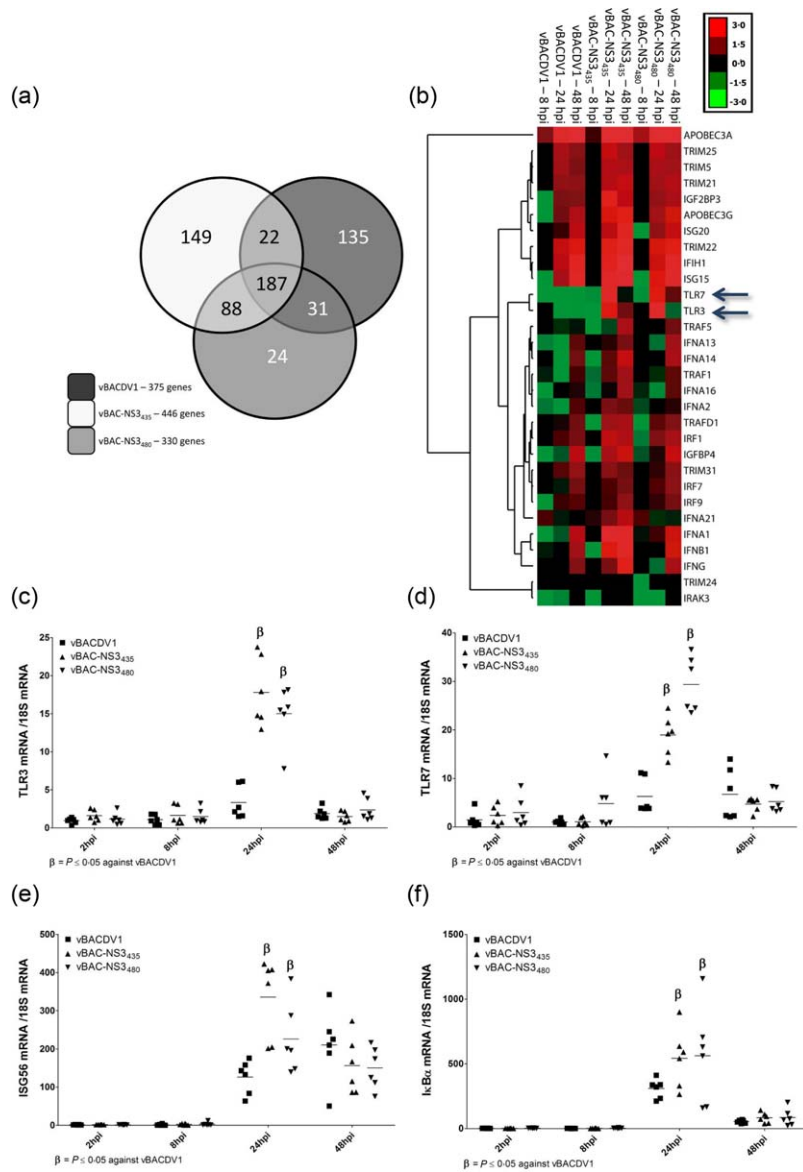


Fig. 2. The Toll-like receptor (TLR)–3 and TLR-7 genes are modulated differentially in monocyte-derived dendritic cells (mdDCs) infected with the dengue virus type 1 (DV1) non-structural protein 3 (NS3)_{hel}-mutated strains. (a) Venn diagram of differential gene expression in mdDCs infected with DV. (b) Hierarchical clustering of the canonical pathway of pattern recognition receptor (PRR) genes that were found to be modulated in the analysis of mRNA microarray data from DV-infected mdDCs. The microarray analysis was performed using mRNA pools from 10 biological replicates. (c) TLR-3 and (d) TLR-7 quantitative reverse transcription–polymerase chain reaction (qRT–PCR) for six cultures of DV-infected mdDCs. The differential expression of ISG56 (e) and IκBα (f) was normalized to the expression of the housekeeping gene 18S in the six mdDC cultures. $\beta = P \leq 0.05$ compared with vBACDV1.

Viral replication can directly trigger DC activation, and can therefore stimulate the production of immunological mediators [44]. In the current study, despite the higher percentage of infected cells (Figs 1b and 3a) and differential gene expression (Fig. 2e,f) in mdDCs infected by the mutated viruses, the secretion of IFN- α was similar to that observed for infection with the parental strain (Fig. 3b). We sought to determine whether the experimental conditions used (MOI of 5) might explain the observed discrepancy. To evaluate whether infection at an MOI of 5 would lead to saturation conditions, with a plateau for IFN- α secretion *in vitro*, mdDCs were infected at an MOI of 1. Higher percentages of infected cells were obtained for DV1-NS3_{hel} mutated viruses compared with the parental strain at 48 hpi (Fig. 3c). Similar results were observed for viral NS3 protein mRNA levels in infected mdDCs (Fig. S7). Interestingly, at the lower MOI of 1 and at later time-

points (24 and 48 hpi), the mutated viruses induced a significant increase in IFN- α secretion in infected mdDCs compared with the parental strain (Fig. 3d). These results suggest a plateau in IFN- α production in mdDCs infected at the MOI used in the previous experiments (MOI of 5) and indicate a direct correlation between viral replication and IFN- α production by infected mdDCs. To confirm this potential plateau in IFN- α production in infected mdDCs, cell cultures were infected with VSV, which induces high amounts of type I IFN. Infection of mdDCs with VSV (Fig. S8) or DV1 (Fig. 3b) at an MOI of 5 induced similar levels of IFN- α secretion, indicating a plateau (i.e. a limited amount of secretion) in the production of this cytokine, depending on the absolute number of cells in the cultures.

To evaluate whether type I IFN would control DV1-NS3_{hel}-mutated virus replication, mdDCs were infected

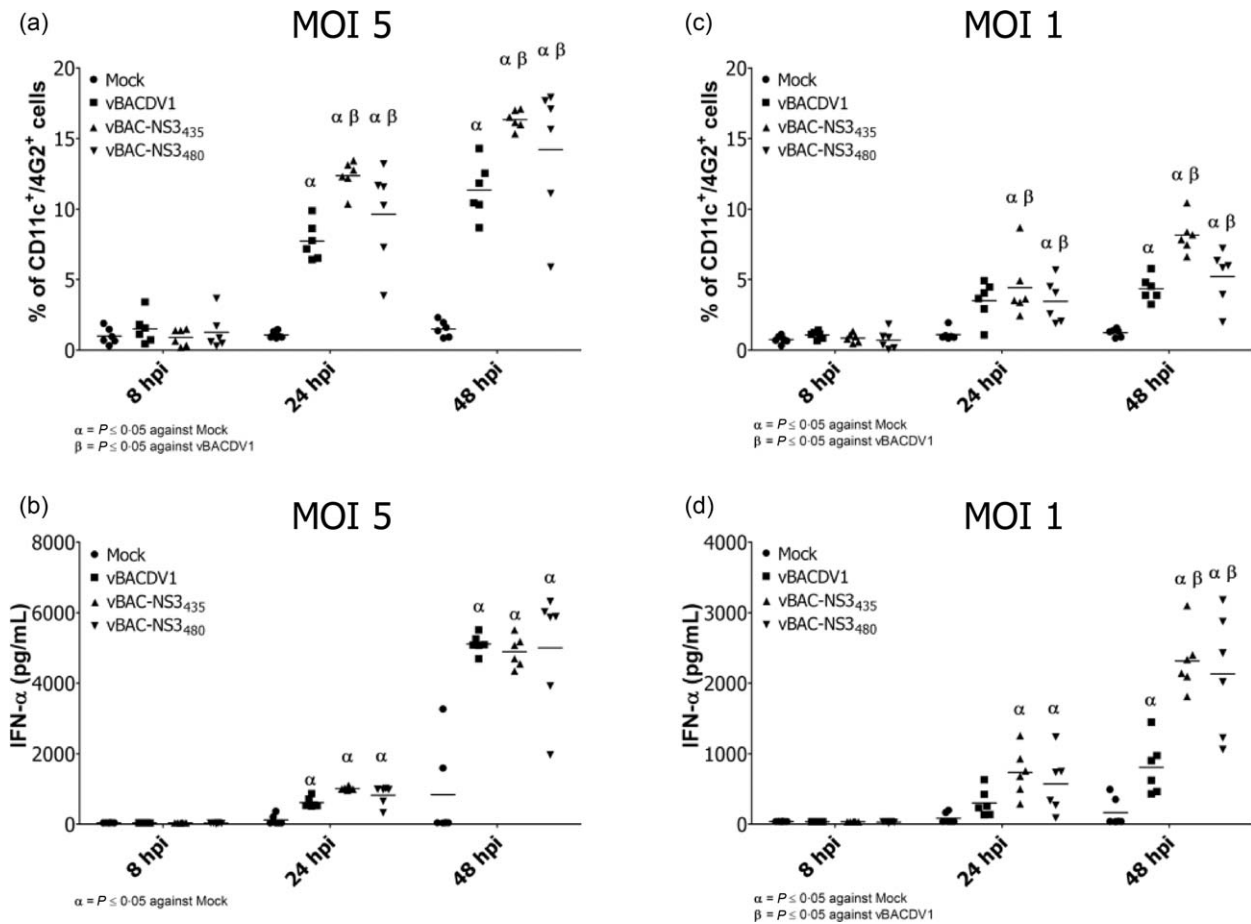


Fig. 3. The multiplicity of infection of dengue virus type 1 (DV1) non-structural protein 3 (NS3)_{hel} mutated strains is associated with differential levels of type I interferon (IFN) secretion by monocyte-derived dendritic cells (mdDCs). A summary of the flow cytometry results for the detection of mdDCs [anti-CD11c monoclonal antibody (mAb)-positive cells] infected with DV (4G2 anti-flavivirus E protein mAb) at a multiplicity of infection (MOI) of 5 (a) or 1 (c). Quantification of IFN- α levels in the supernatants of six cultures of mdDCs infected with DV at an MOI of 5 (b) or 1 (d). $\alpha = P \leq 0.05$ compared with mock; $\beta = P \leq 0.05$ compared with vBACDV1.

(MOI of 5) with vBACDV1, vBAC-NS3₄₃₅ or vBAC-NS3₄₈₀, or mock-infected and treated with rIFN- α or a neutralizing mAb against human IFN α/β receptor chain 2 (α -IFN-R2). The percentage of infection was assessed by flow cytometry assays (Fig. 4). Treatment with rIFN- α reduced the infection rates of the parental virus (Fig. 4a) and the mutated viruses (Fig. 4b,c) significantly, suggesting that DV1 strains cannot block type I IFN function in mdDCs. Additionally, at later time-points, treatment with an α -IFNR2 antibody resulted in increased percentages of positive cells infected with the mutated viruses (Fig. 4b,c). The average percentages of vBAC-NS3₄₃₅-infected cells and vBAC-NS3₄₈₀-infected cells increased from 20 to 50% following treatment with the antibody, reinforcing the notion that IFN- α is able to restrict viral spread and further replication. The levels of IFN- α observed in the supernatant of mdDC cultures were consistent with the treatment data and with our previous experiments (Fig. S9). Taken

together, these results suggest that IFN- α is able to reduce the percentage of mdDC infection by DV1-mutated strains, but due to the high replication rate this decrease is not sufficient to abrogate (or limit) the infection.

Discussion

The nature of the pathophysiological mechanisms triggering DF, the severe forms of dengue (DHF and DSS) and unusual DF manifestations remain unclear. Nevertheless, viral strain characteristics attributable to intrinsically high rates of replication [22] and host immune responses [23,45,46] appear to determine the pathogenesis of dengue. Therefore, it is important to investigate further how viral genetic determinants co-operate with immunological factors and contribute to severe clinical outcomes or protection. Recently, our group demonstrated that the presence of a mutation affecting the DV1-NS3_{hel} protein (L435S or

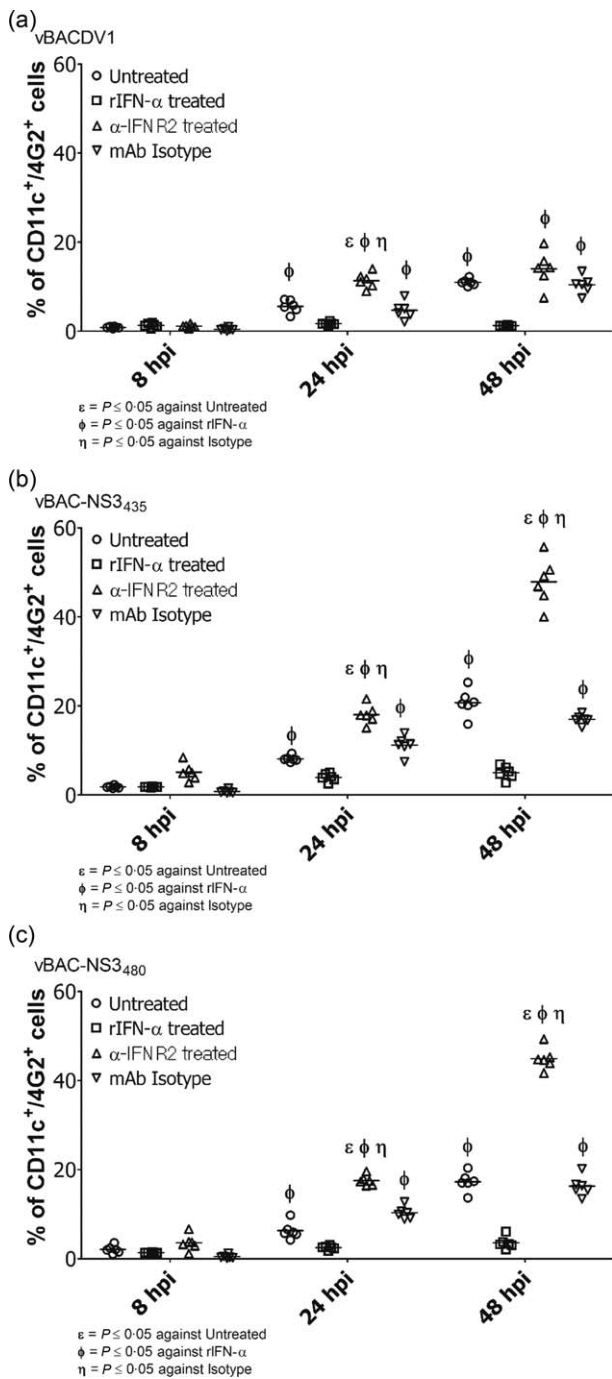


Fig. 4. High type I interferon (IFN) levels are required to eliminate monocyte-derived dendritic cell (mdDC) infection by dengue virus type 1 (DV1) non-structural protein 3 (NS3)_{hel} mutated strains. A summary of the flow cytometry results from six cultures of mdDCs [anti-CD11c monoclonal antibody (mAb)-positive cells] infected with DV (4G2 anti-flavivirus E protein mAb) in the form of vBACDV1 (a), vBAC-NS3435 (b) or vBAC-NS3480 (c). The mdDCs were left untreated (open circle) or were treated with recombinant IFN- α (open squares), the neutralizing monoclonal antibody (mAb) α -IFN R2 (open triangles) or an isotype-control mAb (open triangles under). $\epsilon = P \leq 0.05$ compared with untreated; $\Phi = P \leq 0.05$ compared with rIFN- α ; $\eta = P \leq 0.05$ compared with the isotype control.

L480S) correlates with increased viral replicative capacity both *in vitro* and *in vivo* by increasing RNA synthesis and the viral load, as well as by enhancing the inflammatory profile and mouse mortality [34]. In the present study, we sought to investigate how the same DV1-NS3_{hel}-mutated strains (vBAC-NS3₄₃₅ or vBAC-NS3₄₈₀) could modulate response of the primary targets of DV infection, human mdDCs [47]. Dendritic cells play a key role as an innate immune cell, triggering adaptive immune responses [23,24,45].

We demonstrated that the presence of mutations at the NS3 helicase surface subdomain 2 increased the ATPase activity of both NS3_{hel} mutants by more than 1.7-fold *in vitro*. As NS3 is a multi-functional protein and has at least three different activities (a serine protease domain, an RNA helicase domain and an RNA triphosphatase domain), we assessed if the mutations in the helicase domain could influence the protease activity. The cleavage efficiency of mutants and parental DENV-1 NS2BNS3 proteins was analysed using synthetic substrates and no differences in the proteolytic activity were observed (data not shown). Thereby, these viral genetic markers contribute to viral replicative capacity gains, improving infection and replication rates and increasing viral progeny in human mdDCs by stimulating NS3 ATPase activity without affecting the proteolytic function of the protein. In an attempt to understand the molecular events behind the enhanced ATPase activity of NS3 variants L435S and L480S, we analysed the available crystal structures of NS3 in apo and in several ligands bound states. Interestingly, L435 belongs to a β -hairpin from the subdomain 2 that has been proposed to be important in the dsRNA unwinding mechanism. According to this study, this β -hairpin element could function as a 'helix opener' and a 'stabilizer' of the unwound duplex. Therefore, we can hypothesize that substitution of L435 by a polar residue (Ser) might have an effect on the disruption of base-pair hydrogen bonds of the dsRNA, favouring the NS3 RNA-stimulating ATPase activity. The effect of the L480S mutation on NS3 ATPase activity is more intriguing. According to the structural data available, L480 is located in the linking region between subdomains II and III, far away from the ATP hydrolytic site and, in contrast to L435, is not likely to participate directly in the interaction with the RNA strand. Nevertheless, structural analysis showed that NS3 undergoes major conformational changes upon RNA binding, in particular a reorientation of the protein subdomains [48]. We are tempted to speculate whether a change of residues composition in the subdomains linker could play a role in NS3 structural flexibility and, by consequence, affect the catalytic activity. Matusan *et al.* suggested the importance of selected clusters of charged amino acids outside helicase and ATPase motifs in the DV-2 NS3 helicase region for enzyme activity and viral replication [39]. Besides that, this study demonstrated that mutations abolishing ATPase and helicase activity *in*

in vitro also prevented virus replication and viral yield. It is therefore likely that individual residues that modulate the NS3_{hel} enzymatic activities could establish the relative contribution to virus replication. Based on these findings, we speculate that the modulation of ATPase activity caused by the presence of non-conservative mutations at positions 435 and 480 of the DV1-NS3 protein might play a role in the helicase activity of the enzyme, thus promoting more efficient viral genomic RNA synthesis by the NS5 RNA-dependent RNA polymerase. The Flavivirus life cycle consists of multiple steps involving RNA and both viral and host proteins that mediate important viral activities. Mutations interfering with specific functions of these elements could determine differences in viral replicative capacity, adaptability and pathogenicity. In a recent study, it was observed that benzoxazole inhibits the action of the NS3_{hel} protein in the four DV serotypes, inhibiting DV replication, and that a single point mutation in the NS3 helicase domain could confer resistance to this compound, acting as escape mutant [49].

Recently, studies have evaluated the response of DV-infected cells using microarray technology. The results established substantial activation of innate immune response-related genes, mediated primarily through type I IFN [50–54]. In the present work, global gene expression analyses using cDNA microarrays revealed different levels of genes related to canonical pathways, with major modulation of the PRR and IFN signalling pathways in mdDCs infected with mutated viruses compared with the parental strain. These two pathways are fundamental in the innate immune response, functioning to sense ssRNA and to prevent viral infection/replication [25,26,43]. A detailed analysis of the differentially expressed genes (by microarray and qRT-PCR) in the PRR pathway revealed that the TLR-3 and TLR-7 genes were modulated differentially in mdDCs infected with the DV1-NS3_{hel}-mutated strains. A Gaussian pattern of TLR-3 and TLR-7 gene modulation, with elevated expression at 24 hpi and decreased expression at 48 hpi, was observed specifically. A similar gene expression pattern was verified for IL-6 [55] during mdDC maturation, with high levels of modulation noted at the median time-point. Accordingly, sensing of viral RNA by TLR-3 and TLR-7 can modulate cell susceptibility to DV by inducing the secretion of type I IFN [51,52]. Nasirudeen *et al.* confirmed that human macrophages lacking TLR-3, which is a major receptor involved in the defence against DV, as mediated by IFN- β , were highly susceptible to DV infection [53]. Jüst *et al.* also showed that macrophages or DCs exhibiting the type I IFN receptor-knock-out phenotype were susceptible to infection by DV [54].

To elucidate the type I IFN secretion pattern in mdDCs infected with the DV1 parental strain or a mutated strain, the levels of these cytokines were assessed in culture supernatants. No differential secretion of type I IFN was observed when cells were infected with the parental strain

or a mutated strain at an MOI of 5. A plateau of production might explain this observation; that is, the maximum level of type I IFN secretion may be limited by the number of mdDCs in cultures stimulated with DV. In 1998, Marcus *et al.* observed a plateau in type I IFN secretion using chicken embryo cells infected with VSV, which corroborates our findings [56]. To address this issue, mdDCs were infected with DV at an MOI of 1 ($\times 5$ less than used previously) to assess lower levels of stimulation by viral RNA and viral replication. At this MOI, a significant increase in the IFN- α concentration was obtained in cultures infected with DV1-NS3_{hel}-mutated strains compared with the vBACDV1 parental strain at 48 hpi. This finding indicates that, at a lower level of stimulation, the *in-vitro* cell culture system was not saturated, resulting in elevated production of IFN- α by mdDCs infected with vBAC-NS3₄₃₅ or vBAC-NS3₄₈₀. These data corroborate previous work demonstrating that type I IFN production is dependent upon viral replication but that IFN levels can plateau [56].

To evaluate the role of type I IFN in mdDC susceptibility, infections were conducted before treatment with rIFN- α as well as before type I IFN pathway inhibition via a neutralizing mAb against human IFN receptor 2 (α -IFN-R2). The results demonstrated an important reduction in infected cells after treatment with rIFN- α , and a significant increase in the infection level was observed in mdDCs after treatment with α -IFN-R2, particularly for NS3_{hel}-mutated strains compared with vBACDV1. These data support the notion that type I IFN is able to control the infection of mdDCs by DV, but due to the increased replicative capacity observed in the mutated strains, the IFN produced by the cells during the course of infection is not able to eliminate the viruses. Umareddy *et al.* demonstrated DV strain specificity for the ability to suppress the type I IFN response *in vitro*. Both low- and high-laboratory-passage DV strains, as well as recent clinical isolates, have been used to infect human cell lines. The results have shown that modulation of type I IFN signalling differs, depending on the DV strain [33]. These data reinforce our findings and demonstrate that infection control by type I IFN might vary depending on the DV strain and also expose the complex interplay of DV and host cell factors, which may impact dengue pathogenesis and prophylaxis.

The results presented suggest that the NS3 mutations enhance viral replicative capacity in the mutated strains, leading to bypass of the anti-viral functions of type I IFN via a high rate of virus growth. Furthermore, it has been demonstrated that the enhanced virulence of human and avian influenza A virus (FLUAV) strains and their ability to antagonize IFN induction in virus-infected cells correlate with single amino acid differences in the sequence of the NS1 protein [57]. Grimm *et al.* have also observed that mice lacking the Mx1 gene were more susceptible to infection with the influenza A strain hvPR8 compared with the standard PR8 strain [58]. HvPR8 is more virulent than the

standard strain (PR8), given its enhanced fitness via increased replicative capacity, efficiency in host cell entry and early gene expression, resulting in enhancement of pathogenic infection by counteracting the anti-viral response of the infected host [58].

In this study, we have demonstrated that unique mutations in the viral genome can modify the progress of DV infection in human cells. Single mutations (L435S and L480S) in the DV1-NS3_{hel} protein increase catalytic activity, which is related to the enhancement of viral replicative capacity, thereby strengthening the replication efficiency and consequently the virulence of these viruses. Enhanced replication is followed by increased stimulation of type I IFN production by mdDCs which, in turn, is not capable of abolishing viral infection. These findings unveil the role of single point mutations in DV phenotypes, altering viral replicative capacity and consequently the host innate immune response. These results might contribute to the rational design of effective anti-dengue attenuated vaccines and treatments.

Acknowledgements

The authors are indebted to Maria Eugenia Ribeiro de Camargo and Dr Jörg Kobarg (Laboratório de Micro-arranjos) from Laboratório Nacional de Luz Sincrotron (LNLS/Campinas/SP/Brasil) for technical support for the microarray experiments and to the Program for Technological Development in Tools for Health-PDTIS-FIOCRUZ for use of its facilities. We are thankful to Dr Priscilla F. Wovk from Carlos Chagas Institute—Fiocruz/PR for critical reading of the manuscript. We also acknowledge Dr Samuel Goldenberg (ICC/Fiocruz) for continuous support.

Disclosure

The authors have no conflicts of financial and/or commercial interests to declare.

References

- 1 Murray KO, Rodriguez LF, Herrington E *et al*. Identification of dengue fever cases in Houston, Texas, with evidence of autochthonous transmission between 2003 and 2005. *Vector Borne Zoonotic Dis* 2013; **13**:835–45.
- 2 Bhatt S, Gething PW, Brady OJ *et al*. The global distribution and burden of dengue. *Nature* 2013; **496**:504–7.
- 3 World Health Organization (WHO). Dengue guidelines for diagnosis, treatment, prevention and control. WHO Library Cataloguing-in-Publication Data 2009; **1**:1–147. Available at: <http://www.who.int/tdr/publications/documents/dengue-diagnosis.pdf>. Accessed 28 September 2015.
- 4 Puri B, Nelson W, Porter KR, Henchal EA, Hayes CG. Complete nucleotide sequence analysis of a Western Pacific dengue-1 virus strain. *Virus Genes* 1998; **17**:85–8.

- 5 Rice CM, Lenches EM, Eddy SR, Shin SJ, Sheets RL, Strauss JH. Nucleotide sequence of yellow fever virus: implications for flavivirus gene expression and evolution. *Science* 1985; **229**:726–33.
- 6 Green AM, Beatty PR, Hadjilaou A, Harris E. Innate immunity to dengue virus infection and subversion of antiviral responses. *J Mol Biol* 2014; **426**:1148–60.
- 7 Nemesio H, Palomares-Jerez F, Villalain J. NS4A and NS4B proteins from dengue virus: membranotropic regions. *Biochim Biophys Acta* 2012; **1818**:2818–30.
- 8 Niyomrattanakit P, Winoyanuwattikun P, Chanprapaph S, Angsuthanasombat C, Panyim S, Katzenmeier G. Identification of residues in the dengue virus type 2 NS2B cofactor that are critical for NS3 protease activation. *J Virol* 2004; **78**:13708–16.
- 9 Xie X, Gayen S, Kang C, Yuan Z, Shi PY. Membrane topology and function of dengue virus NS2A protein. *J Virol* 2013; **87**:4609–22.
- 10 Muller DA, Young PR. The flavivirus NS1 protein: molecular and structural biology, immunology, role in pathogenesis and application as a diagnostic biomarker. *Antiviral Res* 2013; **98**:192–208.
- 11 Grun JB, Brinton MA. Dissociation of NS5 from cell fractions containing West Nile virus-specific polymerase activity. *J Virol* 1987; **61**:3641–4.
- 12 Bazan JF, Fletterick RJ. Detection of a trypsin-like serine protease domain in flaviviruses and pestiviruses. *Virology* 1989; **171**:637–9.
- 13 Henchal EA, Putnak JR. The dengue viruses. *Clin Microbiol Rev* 1990; **3**:376–96.
- 14 Liu WJ, Chen HB, Khromykh AA. Molecular and functional analyses of Kunjin virus infectious cDNA clones demonstrate the essential roles for NS2A in virus assembly and for a non-conservative residue in NS3 in RNA replication. *J Virol* 2003; **77**:7804–13.
- 15 Yamshchikov VE, Compans RW. Formation of the flavivirus envelope: role of the viral NS2B-NS3 protease. *J Virol* 1995; **69**:1995–2003.
- 16 Henchal EA, Gentry MK, McCown JM, Brandt WE. Dengue virus-specific and flavivirus group determinants identified with monoclonal antibodies by indirect immunofluorescence. *Am J Trop Med Hyg* 1982; **31**:830–6.
- 17 Casals J, Brown LV. Hemagglutination with arthropod-borne viruses. *J Exp Med* 1954; **99**:429–49.
- 18 Casals J, Brown LV. Hemagglutination with certain arthropod-borne viruses. *Proc Soc Exp Biol Med* 1953; **83**:170–3.
- 19 Kuno G, Chang GJ, Tsuchiya KR, Karabatsos N, Cropp CB. Phylogeny of the genus *Flavivirus*. *J Virol* 1998; **72**:73–83.
- 20 Rothman AL, Ennis FA. Immunopathogenesis of Dengue hemorrhagic fever. *Virology* 1999; **257**:1–6.
- 21 Malavige GN, Fernando S, Fernando DJ, Seneviratne SL. Dengue viral infections. *Postgrad Med J* 2004; **80**:588–601.
- 22 Vaughn DW, Green S, Kalayanarooj S *et al*. Dengue viremia titer, antibody response pattern, and virus serotype correlate with disease severity. *J Infect Dis* 2000; **181**:2–9.
- 23 Dejnirattisai W, Duangchinda T, Lin CL *et al*. A complex interplay among virus, dendritic cells, T cells, and cytokines in dengue virus infections. *J Immunol* 2008; **181**:5865–74.
- 24 Pryor MJ, Carr JM, Hocking H, Davidson AD, Li P, Wright PJ. Replication of dengue virus type 2 in human monocyte-derived macrophages: comparisons of isolates and recombinant viruses with substitutions at amino acid 390 in the envelope glycoprotein. *Am J Trop Med Hyg* 2001; **65**:427–34.

- 25 Bowie AG, Unterholzner L. Viral evasion and subversion of pattern-recognition receptor signalling. *Nat Rev Immunol* 2008; **8**:911–22.
- 26 Pagni S, Fernandez-Sesma A. Evasion of the human innate immune system by dengue virus. *Immunol Res* 2012; **54**:152–9.
- 27 Holm CK, Jensen SB, Jakobsen MR *et al.* Virus–cell fusion as a trigger of innate immunity dependent on the adaptor STING. *Nat Immunol* 2012; **13**:737–43.
- 28 Munoz-Jordan JL, Sanchez-Burgos GG, Laurent-Rolle M, Garcia-Sastre A. Inhibition of interferon signaling by dengue virus. *Proc Natl Acad Sci USA* 2003; **100**:14333–8.
- 29 Rodriguez-Madoz JR, Belicha-Villanueva A, Bernal-Rubio D, Ashour J, Ayllon J, Fernandez-Sesma A. Inhibition of the type I interferon response in human dendritic cells by dengue virus infection requires a catalytically active NS2B3 complex. *J Virol* 2010; **84**:9760–74.
- 30 Yu CY, Chang TH, Liang JJ, Chiang RL, Lee YL, Liao CL *et al.* Dengue virus targets the adaptor protein MITA to subvert host innate immunity. *PLOS Pathog* 2012; **8**:e1002780.
- 31 Ashour J, Laurent-Rolle M, Shi PY, Garcia-Sastre A. NS5 of dengue virus mediates STAT2 binding and degradation. *J Virol* 2009; **83**:5408–18.
- 32 Rajsbaum R, Garcia-Sastre A, Versteeg GA. TRIMmunity: the roles of the TRIM E3-ubiquitin ligase family in innate antiviral immunity. *J Mol Biol* 2014; **426**:1265–84.
- 33 Umareddy I, Tang KF, Vasudevan SG, Devi S, Hibberd ML, Gu F. Dengue virus regulates type I interferon signalling in a strain-dependent manner in human cell lines. *J Gen Virol* 2008; **89**:3052–62.
- 34 de Borja L, Strottmann DM, de Noronha L, Mason PW, Dos Santos CN. Synergistic interactions between the NS3(hel) and E proteins contribute to the virulence of dengue virus type 1. *PLOS Negl Trop Dis* 2012; **6**:e1624.
- 35 Gould EA, Clegg JCS. Growth, titration and purification of togaviruses. In: Mahy BWJ, ed. *Virology: a practical approach*. Washington, DC: IRL Press, 1985; 43–78.
- 36 Silveira GF, Meyer F, Delfraro A *et al.* Dengue virus type 3 isolated from a fatal case with visceral complications induces enhanced proinflammatory responses and apoptosis of human dendritic cells. *J Virol* 2011; **85**:5374–83.
- 37 Irizarry RA, Hobbs B, Collin F, Beazer-Barclay YD, Antonellis KJ, Scherf U *et al.* Exploration, normalization, and summaries of high density oligonucleotide array probe level data. *Biostatistics* 2003; **4**:249–64.
- 38 Livak KJ, Schmittgen TD. Analysis of relative gene expression data using real-time quantitative PCR and the $2(-\Delta\Delta C_t)$ method. *Methods* 2001; **25**:402–8.
- 39 Matusan AE, Pryor MJ, Davidson AD, Wright PJ. Mutagenesis of the Dengue virus type 2 NS3 protein within and outside helicase motifs: effects on enzyme activity and virus replication. *J Virol* 2001; **75**:9633–43.
- 40 Carter SG, Karl DW. Inorganic phosphate assay with malachite green: an improvement and evaluation. *J Biochem Biophys Methods* 1982; **7**:7–13.
- 41 Wang CC, Huang ZS, Chiang PL, Chen CT, Wu HN. Analysis of the nucleoside triphosphatase, RNA triphosphatase, and unwinding activities of the helicase domain of dengue virus NS3 protein. *FEBS Lett* 2009; **583**:691–6.
- 42 Despres P, Frenkiel MP, Ceccaldi PE, Duarte Dos Santos C, Deubel V. Apoptosis in the mouse central nervous system in response to infection with mouse-neurovirulent dengue viruses. *J Virol* 1998; **72**:823–9.
- 43 Wu SJ, Grouard-Vogel G, Sun W *et al.* Human skin Langerhans cells are targets of dengue virus infection. *Nat Med* 2000; **6**:816–20.
- 44 Nightingale ZD, Patkar C, Rothman AL. Viral replication and paracrine effects result in distinct, functional responses of dendritic cells following infection with dengue 2 virus. *J Leukoc Biol* 2008; **84**:1028–38.
- 45 Navarro-Sanchez E, Despres P, Cedillo-Barron L. Innate immune responses to dengue virus. *Arch Med Res* 2005; **36**:425–35.
- 46 Dejnirattisai W, Webb AI, Chan V, Jumnainsong A, Davidson A, Mongkolsapaya J *et al.* Lectin switching during dengue virus infection. *J Infect Dis* 2011; **203**:1775–83.
- 47 Marovich M, Grouard-Vogel G, Louder M *et al.* Human dendritic cells as targets of dengue virus infection. *J Invest Dermatol Symp Proc* 2001; **6**:219–24.
- 48 Luo D, Xu T, Watson RP *et al.* Insights into RNA unwinding and ATP hydrolysis by the flavivirus NS3 protein. *EMBO J* 2008; **27**:3209–19.
- 49 Byrd CM, Grosenbach DW, Berhanu A *et al.* Novel benzoxazole inhibitor of dengue virus replication that targets the NS3 helicase. *Antimicrob Agents Chemother* 2013; **57**:1902–12.
- 50 Qin S, Rottman JB, Myers P *et al.* The chemokine receptors CXCR3 and CCR5 mark subsets of T cells associated with certain inflammatory reactions. *J Clin Invest* 1998; **101**:746–54.
- 51 Sariol CA, Martinez MI, Rivera F *et al.* Decreased dengue replication and an increased anti-viral humoral response with the use of combined Toll-like receptor 3 and 7/8 agonists in macaques. *PLOS ONE* 2011; **6**:e19323.
- 52 Liang Z, Wu S, Li Y *et al.* Activation of Toll-like receptor 3 impairs the dengue virus serotype 2 replication through induction of IFN- β in cultured hepatoma cells. *PLOS ONE* 2011; **6**:e23346.
- 53 Nasirudeen AM, Wong HH, Thien P, Xu S, Lam KP, Liu DX. RIG-I, MDA5 and TLR3 synergistically play an important role in restriction of dengue virus infection. *PLOS Negl Trop Dis* 2011; **5**:e926.
- 54 Züst R, Toh YX, Valdes I *et al.* Type I IFN signals in macrophages and dendritic cells control dengue virus infection: implications for a new mouse model to test dengue vaccines. *J Virol* 2014; **88**:7276–85.
- 55 Blaschkea V, Reicha K, Blaschkeb S, Zippricha S, Neumann C. Rapid quantitation of proinflammatory and chemoattractant cytokine expression in small tissue samples and monocyte-derived dendritic cells: validation of a new real-time RT-PCR technology. *J Immunol Methods* 2000; **246**:79–90.
- 56 Marcus PI, Rodriguez LL, Sekelick MJ. Interferon induction as a quasispecies marker of vesicular stomatitis virus populations. *J Virol* 1998; **72**:542–9.
- 57 Li S, Min JY, Krug RM, Sen GC. Binding of the influenza A virus NS1 protein to PKR mediates the inhibition of its activation by either PACT or double-stranded RNA. *Virology* 2006; **349**:13–21.
- 58 Grimm D, Staeheli P, Hufbauer M *et al.* Replication fitness determines high virulence of influenza A virus in mice carrying functional Mx1 resistance gene. *Proc Natl Acad Sci USA* 2007; **104**:6806–11.

Supporting information

Additional Supporting information may be found in the online version of this article at the publisher's web-site:

Fig. S1. Monocyte-derived dendritic cell (mdDC) phenotype. Expression of molecular markers on the surface of mdDCs in six cultures. Percentages of CD14⁺ (circles), CD1a⁺ (squares), CD11c⁺ (triangles over), CD11b⁺ (triangles under), CD209⁺ (diamonds) and human leucocyte antigen D-related (HLA-DR)⁺ (hexagons) cells. $\alpha = P \leq 0.05$ compared with the isotype control.

Fig. S2. The influence of various recombinant interferon (rIFN)- α concentrations on dengue virus (DV)-infected monocyte-derived dendritic cells (mdDCs). (a) A representative example of a dot-plot for and gating of cells from one of six donors. Flow cytometry determination was performed for six cultures of mdDCs [anti-CD11c monoclonal antibody (mAb)-positive cells] infected with DV (4G2 anti-flavivirus E protein mAb) and either left untreated or treated with 20, 100 or 200 U/ml recombinant interferon (rIFN)- α after infection. (b) A summary of the results for the percentage of mdDCs positive for DV infection, as determined by flow cytometry. $\alpha = P \leq 0.05$ compared with mock; $\beta = P \leq 0.05$ compared with vBACDV1.

Fig. S3. The presence of mutations does not alter the binding affinities of viruses during monocyte-derived dendritic cell (mdDC) infection. A binding assay was performed to define the affinity of dengue virus type 1 (DV1) non-structural protein 3 (NS3)_{hel} mutated viruses for mdDCs. (a) Percentage of mdDCs from six different donors that were positive for DV infection, as determined by flow cytometry. (b) Determination of DV-NS3 mRNA in mdDC pellets. The results are expressed as the fold change (FC) between cells infected with an NS3-mutated strain and mock-infected cells and were normalized to the 18S housekeeping gene using the $2^{-\Delta\Delta CT}$ method. The results are expressed as a ratio of the fold increase at 8 h post-infection (hpi). $\alpha = P \leq 0.05$ compared with mock; $\beta = P \leq 0.05$ compared with vBACDV1.

Fig. S4. Single point mutations at the 435 or 480 position in the dengue virus type 1 (DV1) non-structural protein 3 (NS3)_{hel} protein enhance adenosine triphosphatase (ATPase) activity. (a) Representative sodium dodecyl sulphate-polyacrylamide gel electrophoresis (SDS-PAGE) (13%) showing the expression and purification of the four variants of NS3_{hel}. The gel was stained with Coomassie blue. The molecular mass standard is indicated on the left (sizes in kDa). (b) Initial rates of ATP hydrolysis by NS3_{hel} variants in the presence of 200 nM of dsRNA and different concentrations of ATP. The rates of Pi release from three independent experiments were normalized against the baseline of NS3_{hel} 200Mut, and the data were fitted to the Michaelis–Menten equation by non-linear

regression. The continuous lines are the best-fitting hyperbolas for each ATP concentration.

Fig. S5. Validation of microarray data using biological replicates of monocyte-derived dendritic cells (mdDCs) infected with dengue virus (DV). Myxovirus resistance 1 (MX1), signal transducer and activator of transcription-2 (STAT-2) and eukaryotic translation initiation factor 2-alpha kinase 2 (EIF2ak2) quantitative reverse transcription–polymerase chain reaction (qRT–PCR) in six cultures of DV-infected mdDCs. $\alpha = P \leq 0.05$ compared with mock; $\beta = P \leq 0.05$ compared with vBACDV1.

Fig. S6. Gene expression of pattern recognition receptor (PRR) pathway components in dengue virus (DV)-infected monocyte-derived dendritic cells (mdDCs). (a) Retinoic acid-inducible gene 1 (RIG-I) and (b) melanoma differentiation-associated gene 5 (MDA5) quantitative reverse transcription–polymerase chain reaction (qRT–PCR) in six cultures of DV-infected mdDCs. The results represent relative gene expression, normalized based on the expression of the housekeeping gene 18S in six cultures of mdDCs.

Fig. S7. The fold change in NS3 mRNA at various multiplicities of infection (MOIs) in monocyte-derived dendritic cells (mdDCs). Real-time quantitative polymerase chain reaction (PCR) analyses of the gene expression of the non-structural protein 3 (NS3) viral protein's mRNA in six cultures of mdDCs infected with dengue virus (DV) at an MOI of 5 (a) or 1 (b). $\alpha = P \leq 0.05$ compared with mock; $\beta = P \leq 0.05$ compared with vBACDV1.

Fig. S8. Infection of monocyte-derived dendritic cells (mdDCs) with vesicular stomatitis virus (VSV). (a) Percentage of mdDCs positive for VSV infection by flow cytometry and (b) quantification of interferon (IFN)- α levels in the supernatants of six cultures of dengue virus (DV)-infected mdDCs. $\alpha = P \leq 0.05$ compared with mock.

Fig. S9. Interferon (IFN)- α concentrations in the supernatants of dengue virus (DV)-infected monocyte-derived dendritic cells (mdDCs). A summary of the results for the IFN- α concentrations (pg/ml) in the supernatants of six cultures of DV-infected mdDCs [vBACDV1 (a), vBAC-non-structural protein 3 (NS3)₄₃₅ (b) and vBAC-NS3₄₈₀ (c)]. The mdDCs were left untreated (open circles) or were treated with recombinant IFN- α (200 U/ml) (open squares), the neutralizing monoclonal antibody (mAb) α -IFN-R2 (open triangles over) or an isotype-control mAb (open triangles under). $\epsilon = P \leq 0.05$ compared with untreated; $\Gamma = P \leq 0.05$ compared with α -IFN-R2; $\eta = P \leq 0.05$ compared with the isotype control.

Table S1. Primers names, gene ID, sequences, annealing temperatures, amplicon sizes and cDNA concentrations used in quantitative polymerase chain reaction (qPCR).

Table S2. Description of genes modulated in mdDCs infected with vBACDV1, by comparison with values for the expression in mock-infected monocyte-derived dendritic cells (mdDCs).

Table S3. Description of genes modulated in monocyte-derived dendritic cells (mdDCs) infected with vBAC-NS3₄₃₅,

by comparison with values for the expression in mock-infected mdDCs.

Table S4. Description of genes modulated in monocyte-derived dendritic cells (mdDCs) infected with vBAC-NS3₄₈₀, by comparison with values for the expression in mock-infected mdDCs.